Valorization of the use of Waste Agricultural Materials for the Anodic Oxidation of Amaranth Red (E123) using SS/PbO2 Anodes Elaborated by Pulsed Mode Current

Amina Othmani (othmaniamina@gmail.com)
Universite de Monastir Faculte des Sciences de Monastir https://orcid.org/0000-0003-1787-9683

Research Article

Keywords: Anodic oxidation, Coupling, Biosorption, Luffa cylindrica, Amaranth

Posted Date: February 24th, 2021

DOI: https://doi.org/10.21203/rs.3.rs-230438/v1

Valorization of the use of waste agricultural materials for the anodic oxidation of Amaranth Red (E123) using SS/PbO_2 anodes elaborated by pulsed mode current

Amina Othmani [1*]

1. Faculty of Sciences of Monastir, University of Monastir, Avenue of the Environment, 5019 Monastir, Tunisia

***Corresponding author:** Dr. Amina Othmani; Email:othmaniamina@gmail.com

ORCID ID: https://orcid.org/0000-0003-1787-9683

Abstract

The present paper aims to valorize the use of cheap agricultural waste materials for polluted water decontamination. An evaluation of the efficiency of coupling anodic oxidation (AO) using SS/PbO_2 electrodes with biosorption by *Luffa cylindrica (L.C)* for the removal of Amaranth Red (E123) from aqueous solution was investigated. The effects of pH, contact time, and initial concentration were studied. The regeneration of *L.C* was estimated based on biosorption /desorption tests. The performance of the coupling process was evaluated based on the color, chemical organic carbon (COD), Total organic carbon (TOC) removals, the energy consumed, and the time required for the degradation of Amaranth. A comparison between the efficiency of the AO and the coupling process for the increase of the lifetimes of the anodes used was done. 54.1, 97.8, and 99.9% of 50 $mg.L^{-1}$ of Amaranth were removed respectively after 85, 65, and 50 min by biosorption, AO, and coupling AO with biosorption. An increase in the percentages of COD, TOC, germination indexes (GI), and Amaranth removals were observed when adopting the coupling process. Furthermore, a decrease in the release of Pb^{2+} ions was observed confirming the good stability of the elaborated anodes during the coupling process. Atomic absorption analysis showed that the Pb^{2+} ions reached about 0.020 $mg.L^{-1}$, after the total removal of Amaranth dye (60 min) and 0.051 after (80 min) respectively, for coupling AO with biosorption and the AO process. These values are inferior to those allowed by the Standards. Phytotoxicity tests confirmed the possibility of the reuse of the treated solutions.

Keywords: Anodic oxidation, Coupling, Biosorption, *Luffa cylindrica*, Amaranth

1. Introduction

The discharge of wastewater laden with polluting substances into the receiving environment without or with unsuitable treatment is a cause for growing concern given the undesirable effects; it can have on the environment and the health of living beings (Iloms et al. 2020). The protection of water resources against this growing

pollution is the subject of several research studies for the implementation of more efficient, inexpensive, and environmentally friendly technologies (Othmani et al. 2020b). The decontamination of water resources can have various origins; they can be inorganic or organic (Garcia-Segura et al. 2015). Wastewater is characterized by strong variations in pH, high concentration of organic matter , and high chemical oxygen demand (Choi et al. 2017). Some compounds are easily degradable chemically or biologically, others are recalcitrant to conventional treatment methods and there is a need to seek more adequate treatment systems (Elaissaoui et al. 2016). Up to date, plenty of methods have been used in the cure of contaminated water including cheap alternatives like biosorption and expensive ones like electrochemical processes (Fernandes et al. 2016; Elaissaoui et al. 2019). Electrochemical treatment, especially anodic oxidation, is generally applied for the treatment of refractory organic compounds present in high concentrations (Ghime and Ghosh 2019). It offers a performing ability for wastewater decontamination from a variety of hazardous pollutants (Panizza and Cerisola 2009). However, the electrochemical process depends crucially on the nature and the stability of the electrode used (Othmani et al. 2019). The anodic oxidation can be more effective when using performing electrodes able to produce a large amount of reactive hydroxyl radicals $^{\bullet}OH$ (Nurhayati 2012). In other words, when using a high anode overvoltage of O_2, like PbO_2, SnO_2, TiO_2, RuO_2, IrO_2 , diamond doped with boron supported on Si or Ti (BDD) etc…(Ghime and Ghosh 2019). SS/PbO_2 anodes have a high over potential for oxygen generation combining high conducting ability and performing electrochemical activity (Morsi et al. 2011; Othmani et al. 2019). However, the short lifetime of the deposited layer of PbO_2 into the substrate these last can be one of the main drawbacks of their use (Mohd and Pletcher 2006). In this context, several methods have been devoted to this utility. However, most of them are expensive and required the use of several products and types of equipment. Among the proposed solutions; the doping methods have been successfully applied for enhancing the stability of the elaborated electrodes (Dao et al. 2020). Coupling two efficient processes to enhance the effectiveness of each process alone has been successfully applied. Among the performing coupling processes studied, we can cite coupling ultrasonic cavitation with electrochemical oxidation, which leads to enhance the effectiveness of the studied parameters like the reaction rate, the energy consumed, and the removal efficiency. (Barros et al. 2014). Others have chosen to modify the PbO_2 electrodes with an environmentally friendly conductive carbon black. The results showed an increase of about 24.66% in the removal efficiency of metronidazole compared to the raw PbO_2 electrodes. Furthermore, an improvement in the current efficiency and the generation of hydroxyl radicals was achieved (Wang et al. 2020). Based on the literature most of the solutions proposed for the enhancement of the stability of electrodes based on PbO_2 are oriented for the doping methods. However, more cheap and clean

alternatives can take place for this utility. Among these alternatives the one proposed by (Othmani et al. 2019) who have offered a new alternative based on the use of alternating current (AC) instead of direct current (DC) for the anodic oxidation of methylene blue (MB) using SS/PbO_2 and Pb/PbO_2 electrodes. Results showed an enhancement of the stability of the used electrodes. Furthermore, atomic absorption analysis confirmed the decrease of the release of (Pb^{2+}) ions to much lower values compared to DC and those allowed by the Standards. A year later, the same team has proposed a cheap alternative based on coupling biosorption using *L.C* with AO using SS/PbO_2 anodes. Results showed that 98.7 and 80.02% of MB were removed, respectively, after 60 and 120 min for AC and DC when using the coupling process. Otherwise, 62.84 and 46.87 % of the same dye were removed by the AO process, respectively, after 120 and 180 min for AC and DC (Othmani et al. 2020a). These findings encourage the use of cheap agricultural waste materials for the removal of more hazardous pollutants. According to the literature, the production of azo dyes is estimated at around 350,000 tons per year (Pagga and Brown 1986; Radhakrishnan 2014). In practice, this category of dye is currently the most common. It represents more than 50% of worldwide production (Khadhraoui et al. 2009). During the dyeing procedures, 10-15% of the dyes used in the initial quantities can be lost and discharged without prior treatment in the effluents (Singh and Arora 2011). These latter are carcinogenic and refractory (Bauer et al. 2001; Barros et al. 2014). Therefore, Amaranth Red (E123) was chosen as a model in this study. Many points were studied in the present paper. First, we tried to encourage the use of cheap and abundant agricultural waste materials for hazardous pollutant removal to replace the use of expensive adsorbent. Second, enhance their capacity uptake and reaction speed by coupling biosorption with anodic oxidation. Third, to enhance the lifetime of the elaborated electrodes used and to minimize the generation of Pb^{2+} ions by a safe and economic method based on the coupling process. The characterization of the biosorbent used and the SS/PbO_2 anodes were done using X-ray diffraction (XRD) and scanning electron microscopy (SEM). Quantitative and qualitative characterization of the used *L.C* was reported based on their point zero charges (pHpzc), surface functionality, functional groups, and elementary decomposition. The evaluation of the quality of the treated water after purification was done based on the color, chemical oxygen demand (COD), and total oxygen-carbon (TOC) removals. Finally, the possibility of the reuse of the treated water and the anodes used was evaluated by phytotoxicity tests. The release of Pb^{2+} ions was done measured using atomic absorption spectrophotometry. The possibility of the regeneration of the used *L.C* was done based on biosorption/desorption tests. Finally, a prediction of the possible pathway of the removal of Amaranth dye by AO and AO coupling biosorption was done.

2. Materials and methods

2.1. Preparation of *L.C*

The used *L.C* has a Tunisian origin. It is composed of 54% of cellulose, 11% of lignin, 5% of pectin, 7% of fats and waxes, and 23% hemicelluloses (Othmani et al. 2020b). The preparation of this biosorbent consisted of cutting the fibers finely, washing those last several times to remove all impurities, and drying them at 70°C until the material was completely dried constantly. The dried sample was ground and sieved to obtain a uniform particle size using an electric shifter. The chosen particles have a diameter of 250 μm.

2.2. Elaboration of SS/PbO_2 by pulsed mode current

A plate of stainless steel (SS) of 2 mm thick, with circular geometry and area 12.56 cm^2 were used for the AO process in the presence and absence of *L.C.* The electrodes were then coated with a chemically inert resin (Araldite 50-50); the electrical contact was ensured by a conductive wire protected by a pyrex tube.

The elaboration of SS/PbO_2 electrodes was done in a bath containing 0.5M of HNO_3 (Sigma –Altrich , purity:95%) and 0.5M of $Pb(NO_3)_2$ Panerac Quimica, SA(purity: 99%). A total of 900 pulses (height =30 mA/cm^2, width =1s, relaxation time=5s at zero current) were applied for each anode for 34 min (Naim et al. 2009).

2.3. Schematic of coupling anodic oxidation with biosorption

The experiments used for the Amaranth Red (E123) removal by biosorption has been performed in triplicate in a batch reactor by adding 0.5 g of *L.C* in 0.5 L of Amaranth solution (pH= 2, 7, and 10; C_0=10 $mg.L^{-1}$, T=25°C, and t=100 min). The same experiments were used for the AO coupling biosorption by adding an electrical mounting comprising a DC source and a voltmeter (J=25 $mA.cm^{-2}$). As for the experimental procedure used for the anodic oxidation tests; it has been performed in a batch reactor. The electrochemical cell consisted of a Plexiglas reactor with PbO_2 supported on SS as an anode and SS as a cathode. The surfaces of anodes and cathodes were fixed at 12.56 cm^2 and the inter distance gap between the anode and the cathode was fixed at 2 cm. Table SM-1 presents some properties of Amaranth Red (E123).

The stock solution of Amaranth Red (E123) (purchased from Sigma-Aldric, purity≥ 99.5%) was prepared by dissolving 1 g of the dye in 1 L of distilled water. Test amaranth red solutions were prepared by diluting the stock dye solution.

The desired concentrations were obtained by successive dilution. The adjustment of pH was done using dilute HCl (0.1 M) or NaOH (0.1M) (purity 95–97%) solution before biosorption. During the experiments, concentrations were determined by UV visible spectrophotometer (Perkin Elmer Lamda 25) using quartz cuvettes at λ=520 nm based on the following equation (Elaissaoui et al. 2016)

$$\text{Color removal (\%)} = \frac{(C_0 - C_t)}{C_0} \times 100 \quad (1)$$

Where

C_0 is the initial dye concentration ($mg.L^{-1}$) and C_t is the dye concentration at any time ($mg.L^{-1}$).

2.3.1. Estimation of the retained amount of dye by the *L.C*

The amount of Amaranth retained by the *L.C* was estimated based on Eq.(2) : (Othmani et al. 2020b)

$$Q_e = \frac{C_0 - C_t}{m} \times V \ (mg.g^{-1}) \quad (2)$$

Where

Q_e is the adsorbed quantity at equilibrium time, C_0 and C_t ($mg.L^{-1}$), correspond respectively to the initial and remaining concentration of Amaranth at any time ($mg.L^{-1}$), V is the volume of solution (L) and m is the mass of *L.C* (g). At equilibrium, C_i = to C_e , and Q = Q_e (Kesraoui et al. 2016)

1.3.2. Desorption study

The regeneration of *L.C* was estimated based on a desorption test in different pH media. 3g of the biosorbent obtained after the AO and the AO coupling biosorption of the maximum retained concentration of Amaranth were recovered after use by filtration and dried in an oven. The obtained samples were placed in 0.5 L of distilled water. After that the pH was fixed at 2, 7, and 10 to evaluate the ability of these samples to desorb in different pH media. The desorbed quantity is calculated as follow:

$$\boldsymbol{Q_d = \frac{C \times V}{m}} \quad (3)$$

Where

Q_d is the desorbed amount (mg/g), C is the concentration at each instant t (mg/L), V is the volume of the solution (L), and m is the mass of the fibers (g).

The desorption rates were calculated according to Eq.(4)

$$\mathbf{TD}(\%) = \frac{Q_{de}}{Q_{ae}} \times \mathbf{100} \quad (4)$$

If TD >50%, the retention of Amaranth by the *L.C* is weak which means it is physisorption,

If TD <50% the retention of Amaranth by the *L.C* is important which means it is chemisorption.

The evaluation of all experiments was performed based on various parameters, like chemical Oxygen Demand (COD), Total Organic Carbon (TOC), and Germination Indexes (GI).

2.4. COD and TOC removals

The % COD removal was determined by a photometric method as follow (Barros et al. 2014)

$$COD\ removal\ (\%) = \frac{COD_0 - COD_t}{COD_0} \times 100 \quad (5)$$

COD_0 and COD_t are the initial oxygen chemical demands before and after fixed time t of electrolysis treatment ($mg.L^{-1}$ O_2).

The measure of TOC was determined by a TOC analyzer (HACHIL, 550-TOC-TN model) and the TOC removal was estimated as follow:

$$TOC\ removal\ (\%) = \frac{TOC_0 - TOC}{TOC0} * 100 \quad (6)$$

Where, TOC_0 and TOC_t are respectively the initial total organic carbon before and after fixed time t of electrolysis treatment (ppm C.O.)

2.5. Average current efficiency (ACE)

The quantity of current used during the degradation of the organic matter was estimated based on the ACE calculated according to Eq (7) (Othmani et al. 2019)

$$\text{ACE}\ (\%) = (COD_0 - COD_t) \times \frac{F \cdot V}{8 \cdot I \cdot t} \times 100 \quad (7)$$

Where I: is the applied current (A), t: is the electrolysis time (min), F: is the Faradic constant (96.487 $Cmol^{-1}$), V: is the solution volume (L) and 8 is the number of electrons exchanged per mole of O_2.

2.6. Energy consumption (EC)

The energy consumed (EC) during the electrolysis was estimated as follows (Elaissaoui et al. 2019)

$$\text{EC}\ (KWh \cdot g^{-1}COD) = \frac{I \cdot V \cdot t}{\Delta COD \cdot Vs} \quad (8)$$

Where

I: is the applied constant current (A), V: is ethe average cell potential value volt, t: is the electrolysis time (h), ΔCOD_o: COD are the experimental measurements (g /L O_2), V_s: is the solution volume (L).

2.7. Phtotoxicity tests

The efficiency of the coupling process was evaluated based on the possibility of the reuse of the treated water using SS/PbO_2 anodes. Therefore, a phytotoxicity test was done to test the inhibitory effect of the tested water on the germination and growth potential of lettuce based on the GI (%) calculated as follow:(Louhıchı et al. 2019) The reference is distilled water.

$$\text{GI}\ (\%) = \frac{\text{number of seeds sprouted in the sample}}{\text{number of seeds sprouted in the reference}} * \frac{\text{average length of root in the sample}}{\text{average root length in the reference}} * (100) \quad (9)$$

2.8. Atomic absorption spectrophotometry

The concentration of Pb^{2+} ions released within the solutions after the AO and coupling AO with biosorption was dosed according to the standard method(Perkin 1996); using a Graphite Furnace Atomic Absorption Spectrometry (NovAA800, Analytik Jena GmbH).

2.9. Morphological and structural Characterizations

SEM was performed using a JEOL JSM 5400 scanning microscope after coating them with gold using a JEOL JFC-1199E ion sputtering device for the characterization of *L.C* and without coating for the characterization of the SS/PbO_2 anodes used.

EDS was planned to assess the surface elemental compositions of *L.C* using a JEOL JSM 5400 scanning microscope. EDS was performed after coating them with gold using a JEOL JFC-1199E ion sputtering device.

XRD characterizations of the elaborated SS/PbO_2 anodes were done using an X-ray diffractometer D8 Advance (Bruker, (CNRSM)) and a Diano, Ka Co radiation at a wavelength of 1.54 nm using the Debye method (Holzwarth and Gibson 2011).

3. Results and discussion

3.1. Surface characterization of *L.C* and SS/PbO_2 anodes

The performance of the biosorption process is depending on the chemical, structural, morphological, and surface properties of the used biosorbent (Adewuyi 2020). Thus, having an idea about the surface of biosorbent used can facilitate the prediction of the main reactions that may occur during the removal of Amaranth dye by biosorption and bisorption coupling AO. According to (Othmani et al. 2020b), *L.C* fibers have an amphoteric character based on their zero charge point (pH_{PZC}) which is equal to 7.38 ±0.0002 . These findings were confirmed by the chemical surface properties of these fibers determined by Boehm titration. Results have shown an affinity between the acidic function and the basic one, where they reached respectively (1.510 ± 0.005, and 1.560 ± 0.0008) ($\times 10^{-4}$mmol/g). The identification of the surface functionally of the used *L.C* will enhance the deep understanding of the main mechanism that may occur during the retention of the Amaranth dye. On the other hand, and according to results found by EDS illustrated in Table 1, *L.C* is mainly composed of Carbone (54.46% of C), and Oxygen (40.6% of O). These high percentages of these compounds suggest the existence of C-O and C=O groups specific to aromatic ring type and alcoholic function. Furthermore, some impurities in low concentration are also present as shown in table SM-2.

As for the SEM micrograph shown in Fig.1, it showed that the *L.C* presents a rough porous structure and a homogeneous appearance which is formed by bonded multicellular fibers (Boynard and D'Almeida 2000). Therefore, this porous structure of *L.C* leads to the retention of Amaranth Red (E123).

3.2. SEM and XRD characterizations of SS/PbO_2 anodes

Fig.2 specific to the XRD and SEM of SS/PbO_2 anodes shows the presence of small crystalline particles and pyramidal ones (Li et al. 2016) attributed respectively to α-PbO_2 form and β-PbO_2 specific to electronic conduction and electrochemical reduction capacity (Zhou and Gao 2007; Othmani et al. 2019).

3.3. Effect of pH

The effect of pH on the removal of Amaranth Red (E123) by biosorption, AO, and biosorption coupling AO was studied over a pH of 2, 7, and 10 as shown in Fig.3. As said earlier, the pH_{PZC} of *L.C* =7.38, therefore the surface of *L.C* is positively charged at pH values below pH_{PZC} and should be able to adsorb negatively charged species. At the same time at pH values above 7.38 *L.C* can adsorb positively charged species (Mbarki et al. 2020) . The best results for AO, biosorption , and coupling AO with biosorption were obtained for pH =2 and reached respectively, 97.8, 54, and 98.7% which can be explained as follow: As the Amaranth Red (E123) is an anionic azo dye with predominantly negative charges at acidic pH (Ahmad and Kumar 2011) and based on the fact that for pH under 7.38, the dominant functional groups of *L.C* are positively charged and therefore attract strongly the negatively charged species. However, with the increase in pH to 7 and 10, the surface of *L.C* becomes more negative and therefore the attraction between the adsorbate and the *L.C* decreased gradually resulting in a decrease in the % of removal of Amaranth. For pH=10 the low % of Amaranth removal can be due to the presence of an excess of OH^- in the solution. This last can enter into competition with the adsorbate for the available sites onto the *L.C* and therefore decline the uptake capacity. For the AO of Amaranth Red (E123), the efficiency of the process was more accentuated for pH=2. The electrolysis is controlled by material transport and side reactions (such as the evolution of oxygen) which begin with the oxidation of amaranth. However, these reactions can also produce other oxidants capable of contributing to the oxidation process and therefore of participating in the mineralization of pollutants. According to the literature, two main parameters strongly influence the electrochemical degradation of Amaranth ; the type of electrolyte used in the electrochemical cell and the solution pH (Barros et al. 2014). As the best results were obtained at pH=2, the possible pathway of the Amaranth Red (E123) degradation can be described as follow: The degradation of the Amaranth molecule by the $^{\cdot}OH$ radical oxidation generated by the SS/PbO_2 anodes starts by the division of N=N– bond, which produces aromatic molecules of lower molecular weight (Silva et al. 2008). According to previous studies, the main

byproducts generated are two primary amines (Zhang et al. 2009) and some oxidation products detected during the mineralization of aromatic compounds like phenol, quinone, malonic, and oxalic acid (Pogacean et al. 2018). Concerning the coupling process, a combination between the possible pathway of the retention of Amaranth dye onto the available sites of *L.C* and the electrochemical degradation of this last has taken place in harmony. Therefore, the removal of Amaranth was faster than each process alone. The presence of *L.C* has given some relaxation time for the SS/PbO_2 anodes which decreased the energy consumed and the mass loss of Pb^{2+} into the solution. This behavior has minimized one of the main drawbacks of the use of anodes based on PbO_2 which is the toxicity generated during the electrolysis. Furthermore, a decrease in the required time for the removal of Amaranth dye was observed indicating the efficiency of the coupling process. These findings must be confirmed by the adsorption atomic analysis, SEM, and SRX analysis of SS/PbO_2 anodes after use.

3.4. Effect of concentration

The effect of concentration on the removal of Amaranth Red (E123) by biosorption in batch mode, AO and AO coupling biosorption was evaluated over a range between [10-100] $mg.L^{-1}$, pH=2, C_{Na2SO4}=0.1M, J=25 mA/cm^2, $m_{L.C}$=0.5g, V=0.5 L, T=25°C, and t=100 min. As shown in Fig.4, the effect of concentration influences differently the removal of Amaranth Red (E123) when adopting the AO, the biosorption, and the coupling process. For the biosorption process, the increase in the initial concentration from 10 to 100 $mg.L^{-1}$ has shown two main phases. An increase in the % of Amaranth removal until reaching 50 $mg.L^{-1}$, indicating fast removal phase; indicating a rise in the number of ions in solution involving a higher biosorption capacity (Othmani et al. 2017). However, for concentration higher than 50 $mg.L^{-1}$, a gradual decrease in the removal efficiency was observed indicating a decrease in the capacity uptakes of the used *L.C* confirmed by the slowdown of the removal speed. Therefore, up to 50 $mg.L^{-1}$ of Amaranth, a relation of proportionality was obtained between the initial concentration and the removal efficiency. These findings can be explained by the decrease in the number of the available sites onto the *L.C* (Othmani et al. 2020a). Therefore, the maximum biosorption capacity of phenol with raw *L.C* is fixed to 50 $mg.L^{-1}$; and the saturation phase was fixed at 85 min (Shahryari et al. 2010). Also, the accumulation of Amaranth on the surface of *L.C* can be another reason for the decline in the removal efficiency (Othmani et al. 2020b). Furthermore , researchers have explained the fast removal speed of the pollutant at the first stage of biosorption to the transfer of external mass and the slow one to the phenomenon of diffusion (internal mass transfer) (Ghaedi et al. 2014; Liu et al. 2018). As for the AO process the same behavior was observed for the removal of Amaranth dye where the maximum % of removal was observed for a concentration of 50 $mg.L^{-1}$ after 65 min. The increase in concentration leads to a decrease in process efficiency.

The degradation of Amaranth Red (E123) was promoted by the hydroxyl radicals formed at the SS/PbO_2 surface from the water oxidation and other weak oxidizing species formed in the sulphate medium. The efficiency of the process depends mainly on the ability of the SS/PbO_2 anodes to produce •OH reagents (Skoumal et al. 2008). The electrochemical oxidation of Amaranth Red (E123) can be divided into two main stages (Baddouh et al. 2019); the first one consists of the formation of hydroxyl radicals ($OH^•$), which is evolved at the anode (M= SS/PbO_2) upon water discharge reaction (Eq.(10))

$$M + H_2O \rightarrow M(OH^•) + H^+ + e^- \quad (10)$$

In the second stage the ($OH^•$) radical adsorbed on the surface of SSPbO_2 anodes as shown in (Equation 10) and hence the hydroxyl radical oxidized the Amaranth molecules.

$$R + M(OH^•) \rightarrow M + RO + H^+ + e^- \quad (11)$$

R: organic compound (Amaranth Red (E123)

The increase of the performance of the AO at first stages until reaching the concentration of 50 $mg.L^{-1}$ can be due to the association of Amaranth Red (E123) molecules to form clusters of low diffusivity; this lowers the rate of pollutant diffusion to the surface of SS/PbO_2 anodes. However, the decrease in the rate of hydroxyl radical's formation leads to a decrease in the rate of Amaranth oxidation. Therefore, the % of dye removal decreases. Similar behavior was observed by (Baddouh et al. 2019) for the removal of MB by AO SnO_2 anodes. As for coupling AO with biosorption the variation of the effect of concentration is similar to each process alone. Both processes have taken place; the presence of DC has played two main roles. At the initial stage of the coupling process, it increased the speed of the fixation of Amaranth dye onto the available sites of *L.C*; the presence of the electric field has increased the disorder in the solution and consequently the mobility of the Amaranth molecules which increased the electrostatic interaction between these last and the functional groups of *L.C*, and therefore, favored their retention by the *L.C*. When the entire available sites were full, DC placed his initial role for the AO process, thus it favored the contact between the SS/PbO_2 anodes and the target molecules and accelerated the production of •OH, which was week at the initial stage due to the presence of a large number of vacant sites onto the biosorbent surface. These findings can be affirmed by the dissolution of Pb^{2+} during the electrolysis process by the absorption atomic analysis.

3.5. Evaluation of the efficiency of the AO and coupling AO with biosorption for the removal of Amaranth: Calculation of % of color, ACE, EC, TOC, and COD removals

Both AO and coupling AO with biosorption by *L.C* for the removal of Amaranth dye were evaluated based on the ability to remove the color, COD, TOC and the variation of ACE, and the EC.

Based on results illustrated in Fig.5.a,b, and c; TOC, COD, and color removals have shown the same variation, an increase in the percentages of removal was observed indicating the performance of both processes. However, the variation of the average current efficiency (ACE) which presents the fraction of current required for the degradation of Amaranth and its sub-products, and the energy consumed (EC) have shown different variations as shown in Fig.5.d; a gradual increase over the time was observed for the EC by both processes used for the removal of Amaranth. However, results achieved for the coupling process were better than those obtained for the AO. The EC passed from (0.07 to 0.29) $\times 10^3$ and from (0.09 to 0.56) $\times 10^3$ (kWh. g^{-1}COD) respectively, for the coupling process and the AO. The variation of ACE was inversely proportional to the variation of EC. As seen in Fig .5.e, specific to the variation of % ACE; a decline in ACE was observed as a function of the electrolysis time for both processes indicating the presence of secondary reactions including the oxygen evolution. Similar findings were obtained in the literature where some researchers have attributed this variation to the formation of refractory products and the decrease in the organic matter (Panizza and Cerisola 2005; Steter et al. 2014; Sasidharan Pillai and Gupta 2015). Moreover, these percentages are lower in the case of the coupling process which confirmed the positive effect played by the *L.C* which decreased the secondary reactions and the possible by-produced produced during the reaction. These findings can be explained more by the germinations tests and the atomic absorption analysis which will test the toxicity of the solutions treated.

3.6. Evaluation of the quality of the treated water

3.6.1. Germination tests

The performance of biosorption, AO, and biosorption coupling with OA was evaluated by phytotoxicity tests of the raw and treated Amaranth solution was carried out using the germination test of *Lactuca Sativa* seeds. A concentration of 10 mg.L^{-1} was chosen for a pH = 2, T=25°C, and after treatment of 80 min. The germination inhibition results obtained are shown in Fig.6. The reference is distilled water. As seen the initial germination index (GI) of Amaranth dye is 35%, an increase in this value was observed after the removal of this dye by biosorption, AO, and coupling AO with biosorption. The GI% has reached about 86% higher than the other processes, which presented a predicted result since biosorption is safe and environmentally friendly. As for the AO, it reached about 54% and for the coupling process about 72%. These findings indicated that the entire percentages are higher than 50% and therefore decay in the toxicity of the tested solutions was achieved (Buchmann et al. 2014). Furthermore, these rates confirmed the decrease in the amounts of by-products formed by the oxidation of amaranth on the SS/PbO_2 anodes (Elaissaoui et al. 2016). The high values reached in the case of the coupling process compared to the AO can be explained by the positive effect played by the *L.C* which

favored the retention of Amaranth by the available sites on its surface and therefore minimize the amount of the by-products formed. Similar behavior was observed for the removal of methylene blue when using the same process (Othmani et al. 2020a).

3.6.1. Atomic Absorption

Dealing with results registered in table SM-2, the presence of detectable Pb^{2+} in solution begins before 50 and 20 min of the total degradation of Amaranth respectively for the AO the coupling process. These findings emphasized the positive effect plays by the *L.C* which enhanced the stability of the anodes by decreasing the contact between these last and the Amaranth and favoring at the same time the retention of the major concentration of this dye. These observations confirmed the explanation given for the effect of concentration on the removal of Amaranth from the solution. Therefore, coupling AO with biosorption by *L.C* fibers can offer a performing alternative for the removal of hazardous pollutants by cheap and safe alternative. The Pb^{2+} ions reached about 0.020 (±0,002 $mg.L^{-1}$), after the total removal of Amaranth dye (60 min) and 0.051(±0,002 $mg.L^{-1}$) after (80 min) respectively, for coupling AO with biosorption and the AO process. These values are lower than those allowed by the Tunisian Standards (NT 106.02, 1989).

3.7. Test of the efficiency of the coupling process on the stability of the SS/PbO_2 anodes

The efficiency of the SS/PbO_2 anodes is linked to the stability of oxide layers during electrolysis. Generally, PbO_2 electrodes have a major drawback which is the deposit corrosion; this corrosion can lead to a loss of efficiency of the electrode. To evaluate the efficiency of the AO and the coupling process on the increase of the lifetime of the SS/PbO_2 anodes during the removal of Amaranth dye, SEM and XRD characterizations after the use of anodes were performed. As seen in Fig.7.a after the use of SS/PbO_2 anodes for the AO of Amaranth, the SEM image of SS/PbO_2 anodes shows the same structure showed before use with the appearance of some big holes specific to the detachment of the PbO_2 layer from the substrate. As for the SEM image specific to the anodes used for the coupling process (Fig.7.b), it shows two different parts like it are divided into two different aspects, indicating a heterogeneous structure due to the electrolysis treatment, and this can ensure that both processes have taken place for the removal of the Amaranth dye in the case of the coupling process. Based on these SEM images and XRD diffractograms, it well noticed that the coupling process has enhanced the stability of the deposed PbO_2 layer on the SS substrate due to the relaxation time offered to the used anodes by the biosorption process which decreased the contact between the Amaranth dye with the anodes and favor their retention by the dominant positively charged sites of *L.C*. These findings can explain the extinction of the major electronic conduction and electrochemical reduction peaks of PbO_2 as shown in the specific diffractogram

obtained for the anodes after the removal of Amaranth by AO. Therefore, we can confirm the effectiveness of the coupling process on the increase of the stability of the anodes used.

3.8. *L.C* regeneration studies

The regeneration ability of the used *L.C* through three consecutive biosorption/desorption cycles was performed for a biosorbent mass of 3 g, an initial concentration of Amaranth of 10 $mg.L^{-1}$, V=0.5 L, and T=25°C.Tests were carried out at different pH media; 2, 7, and 10. Based on Fig.8, the best desorption was obtained at pH=2 for the biosorption and biosorption coupling AO. As seen, at pH 7 and 10 all the desorption rates for the three cycles were higher than 50% indicating that the retention forces of Amaranth by the *L.C* for both processes and during the three cycles are weak . Thus at neutral and basic pH, the biosorption of Amaranth is physisorption (Inyinbor et al. 2015). In other words, the linkages are Van Der Walls which can explain the easiness of the desorption. Of course, the rates are approximatively the same with very low experimental, errors since we have the same number of sites and the capacity uptake is the same. At pH=2, all the desorption rates obtained for the biosorption and the biosorption coupling AO were lower than 50% confirming that the retention forces of Amaranth by both processes are strong and therefore it is chemisorption. In this case, the biosorption mechanisms involved in this retention may be hydrogen-bonding formations, and n–π interaction (Tran et al. 2017). As seen after the desorption rates decreased slowly after three cycles of biosorption/desorption of Amaranth dye by biosorption and biosorption coupling AO. It appears that the times required for the saturation for the biosorption and biosorption coupling AO decreased by increasing the number of regeneration cycles which can be dependent on the gradual decrease of the biosorption capacity from the first to the third cycle. Despite this gradual decrease, these findings confirmed the good regeneration ability of the used *L.C* even after three continuous cycles.

3.9 A comparative study with reported literature

The success of the alternative offered for the enhancement of the deposited PbO_2 layer on the target substrate cannot be confirmed without comparing the main achievement with those illustrated in previous studies Therefore, a comparative study of the stability of the PbO_2 layer onto a different substrate and their performance for the degradation of some pollutants was given in the table SM-3. Based on the results collected coupling AO using SS/PbO_2 anodes with biosorption by *L.C* has shown similar efficacity to those reached after doping the anodes used.

3.9. Possible pathway for the removal of Amaranth dye by coupling AO with biosorption

An assumption of the pathway of the removal of Amaranth by the AO and coupling AO with biosorption was proposed. Based on the literature the possible pathway for the degradation of Amaranth dye by AO under DC is

384 divided into two main steps: the first one as described in Fig.8 is specific to the formation of hydroxyl radicals
385 which is evolved at SS/PbO_2 anodes upon water discharge reaction, after that the hydroxyl radicals will be
386 adsorbed on the surface of the used anodes. The second step consists of the oxidation of the Amaranth dye by
387 these last. As for the coupling process, and based on results obtained during this study, the mechanism can be
388 divided into two stages. The first one is specific to the fixation of the Amaranth onto the available sites onto the
389 surface of *L.C* until the saturation phase. As the dominant functional groups onto the *L.C* are positively charged,
390 the main pathway of the fixation of Amaranth is the electrostatic interaction (especially that the Amaranth is
391 negatively charged at pH =2). The second one is specific to the AO process were the same mechanism that is
392 described before has taken place for the degradation of the remaining molecules of Amaranth dye.

393 **4. Conclusions**

394 Coupling anodic oxidation using SS/PbO_2 anodes electrodeposited by pulsed mode current with biosorption
395 by *Luffa cylindrica* has offered a cheap and effective alternative for the removal of Amaranth Red (E123) from
396 aqueous solution. The combination of both processes has enhanced the stability of the electrodeposited layer of
397 PbO_2 on the SS substrate giving similar performance to that of the doping methods. The results showed that the
398 presence of biosorbent allowed the retention of Amaranth by their available vacant sites which minimize the
399 dissolution of Pb^{2+} ions, increase the percentages of removal of Amaranth and decrease the required time for the
400 purification. During the coupling process direct current has played two main roles; it increased the contact
401 between the opposites charged species in solution which accelerated their retention of Amaranth dye by the
402 biosorbent used and enhanced the production of hydroxyl radicals which favors the degradation of the target
403 pollutant. The biosorption/desorption confirmed the good regeneration ability of the used *L.C* even after three
404 continuous cycles. Atomic absorption analysis confirmed the respect of the obtained concentrations of Pb^{2+} to
405 the Standards. The phytotoxicity tests confirmed the possibility of the reuse of the treated water where all the
406 germination indexes are higher than 50%. Therefore the sub-products produced during the degradation of
407 Amaranth dye are mineralized as confirmed by the high values of COT and COD. Thus the treated solutions can
408 load to any receiving water.

409 **Acknowledgment**

410 D.r Amina expresses her sincere gratitude to the staff of the Faculty of science of Gafsa, Faculty of science of
411 Monastir, and the company of Phosphate of Gafsa for their help throughout her study.

412 **Conflict of interest**

413 The present paper is an original work with no conflict of interest of any kind.

Ethical Approval: Dr Amina Othmani confirms that this work is original and has not been published elsewhere nor is it currently under consideration for publication elsewhere.

Consent to Participate: Not applicable.

Consent to Publish: Dr Amina Othmani agrees to publish this work.

Authors Contributions: The conceptualization, methodology, writing- original draft preparation, and editing were done by Dr Amina Othmani

Funding: Dr Amina Othmani declares that she has no known competing financial interests or personal relationships that could have appeared to influence the work reported in this paper.

Availability of data and materials: Applicable.

References

Adewuyi A (2020) Chemically modified biosorbents and their role in the removal of emerging pharmaceuticalwaste in the water system. Water (Switzerland) 12:1–31. https://doi.org/10.3390/W12061551

Ahmad R, Kumar R (2011) Adsorption of Amaranth Dye onto Alumina Reinforced Polystyrene. Clean - Soil, Air, Water 39:74–82. https://doi.org/10.1002/clen.201000125

Baddouh A, Rguiti MM, El Ibrahimi B, et al (2019) Anodic oxidation of methylene blue dye from aqueous solution using sno2 electrode. Iran J Chem Chem Eng 38:175–184

Barros WRP, Steter JR, Lanza MRV, Motheo AJ (2014) Degradation of amaranth dye in alkaline medium by ultrasonic cavitation coupled with electrochemical oxidation using a boron-doped diamond anode. Electrochim Acta 143:180–187. https://doi.org/10.1016/j.electacta.2014.07.141

Bauer C, Jacques P, Kalt A (2001) Photooxidation of an azo dye induced by visible light incident on the surface of TiO2. J Photochem Photobiol A Chem 140:87–92. https://doi.org/10.1016/S1010-6030(01)00391-4

Boynard CA, D'Almeida JRM (2000) Morphological characterization and mechanical behavior of sponge gourd (Luffa cylindrica)-polyester composite materials. Polym - Plast Technol Eng 39:489–499. https://doi.org/10.1081/PPT-100100042

Buchmann C, Felten A, Peikert B, et al (2014) Development of phytotoxicity and composition of a soil treated with olive mill wastewater (OMW): an incubation study. Plant Soil 386:99–112. https://doi.org/10.1007/s11104-014-2241-3

Choi YY, Baek SR, Kim JI, et al (2017) Characteristics and biodegradability of wastewater organic matter in municipal wastewater treatment plants collecting domestic wastewater and industrial discharge. Water

(Switzerland) 9:. https://doi.org/10.3390/w9060409

Dao KC, Yang CC, Chen KF, Tsai YP (2020) Recent trends in removal pharmaceuticals and personal care products by electrochemical oxidation and combined systems. Water (Switzerland) 12:. https://doi.org/10.3390/W12041043

Elaissaoui I, Akrout H, Grassini S, et al (2016) Role of SiOx interlayer in the electrochemical degradation of Amaranth dye using SS/PbO2 anodes. Mater Des 110:633–643. https://doi.org/10.1016/j.matdes.2016.08.044

Elaissaoui I, Akrout H, Grassini S, et al (2019) Effect of coating method on the structure and properties of a novel PbO2 anode for electrochemical oxidation of Amaranth dye. Chemosphere 217:26–34. https://doi.org/10.1016/j.chemosphere.2018.10.161

Fernandes A, Santos D, Pacheco MJ, et al (2016) Electrochemical oxidation of humic acid and sanitary landfill leachate: Influence of anode material, chloride concentration and current density. Sci Total Environ 541:282–291. https://doi.org/10.1016/j.scitotenv.2015.09.052

Garcia-Segura S, Keller J, Brillas E, Radjenovic J (2015) Removal of organic contaminants from secondary effluent by anodic oxidation with a boron-doped diamond anode as tertiary treatment. J Hazard Mater 283:551–557. https://doi.org/10.1016/j.jhazmat.2014.10.003

Ghaedi M, Nasab AG, Khodadoust S, et al (2014) Application of activated carbon as adsorbents for efficient removal of methylene blue: Kinetics and equilibrium study. J Ind Eng Chem 20:2317–2324. https://doi.org/10.1016/j.jiec.2013.10.007

Ghime D, Ghosh P (2019) Removal of Organic Compounds Found in the Wastewater through Electrochemical Advanced Oxidation Processes: A Review. Russ J Electrochem 55:591–620. https://doi.org/10.1134/S1023193519050057

Holzwarth U, Gibson N (2011) The Scherrer equation versus the “Debye-Scherrer equation.” Nat Nanotechnol 6:534. https://doi.org/10.1038/nnano.2011.145

Iloms E, Ololade OO, Ogola HJO, Selvarajan R (2020) Investigating industrial effluent impact on municipal wastewater treatment plant in vaal, South Africa. Int J Environ Res Public Health 17:1–18. https://doi.org/10.3390/ijerph17031096

Inyinbor AA, Adekola FA, Olatunji GA (2015) Adsorption of rhodamine b dye from aqueous solution on Irvingia gabonensis biomass: Kinetics and thermodynamics studies. South African J Chem 68:115–125. https://doi.org/10.17159/0379-4350/2015/v68a17

Kesraoui A, Moussa A, Ali G Ben, Seffen M (2016) Biosorption of alpacide blue from aqueous solution by lignocellulosic biomass: Luffa cylindrica fibers. Environ Sci Pollut Res 23:15832–15840. https://doi.org/10.1007/s11356-015-5262-4

Khadhraoui M, Trabelsi H, Ksibi M, et al (2009) Discoloration and detoxicification of a Congo red dye solution by means of ozone treatment for a possible water reuse. J Hazard Mater 161:974–981. https://doi.org/10.1016/j.jhazmat.2008.04.060

Li X, Xu H, Yan W (2016) Fabrication and characterization of PbO 2 electrode modified with polyvinylidene fluoride (PVDF). Appl Surf Sci 389:278–286. https://doi.org/10.1016/j.apsusc.2016.07.123

Liu Y, Chen J, Cui B, et al (2018) Design and Preparation of Biomass-Derived Carbon Materials for Supercapacitors: A Review. C 4:53. https://doi.org/10.3390/c4040053

Louhıchı G, Bousselmı L, Ghrabı A, Khounı I (2019) Process optimization via response surface methodology in the physico-chemical treatment of vegetable oil refinery wastewater. Environ Sci Pollut Res 26:18993–19011. https://doi.org/10.1007/s11356-018-2657-z

Mbarki F, Othmani A, Kesraoui A, Seffen M (2020) Coupling alternating current and biosorption for the removal of hexavalent chromium. Chem Eng Technol 1–11. https://doi.org/10.1002/ceat.202000398

Mohd Y, Pletcher D (2006) The fabrication of lead dioxide layers on a titanium substrate. Electrochim Acta 52:786–793. https://doi.org/10.1016/j.electacta.2006.06.013

Morsi MS, Al-Sarawy AA, El-Dein WAS (2011) Electrochemical degradation of some organic dyes by electrochemical oxidation on a pb/pbo2 electrode. Desalin Water Treat 26:301–308. https://doi.org/10.5004/dwt.2011.1926

Naim MN, Kuwata M, Kamiya H, Lenggoro IW (2009) Deposition of TiO2 nanoparticles in surfactant-containing aqueous suspension by a pulsed DC charging-mode electrophoresis. J Ceram Soc Japan 117:127–132. https://doi.org/10.2109/jcersj2.117.127

Nurhayati E (2012) A Brief Review on Electro-generated Hydroxyl Radical for Organic Wastewater Mineralization. J Sains &Teknologi Lingkung 4:24–31. https://doi.org/10.20885/jstl.vol4.iss1.art3

Othmani A, Kesraoui A, Akrout H, et al (2019) Use of alternating current for colored water purification by anodic oxidation with SS/PbO2 and Pb/PbO2 electrodes. Environ Sci Pollut Res 26:25969–25984. https://doi.org/10.1007/s11356-019-05722-w

Othmani A, Kesraoui A, Akrout H, et al (2020a) Coupling anodic oxidation, biosorption and alternating current as alternative for wastewater purification. Chemosphere 249:126480.

504 https://doi.org/10.1016/j.chemosphere.2020.126480
505 Othmani A, Kesraoui A, Seffen M (2017) The alternating and direct current effect on the elimination of cationic
506 and anionic dye from aqueous solutions by electrocoagulation and coagulation flocculation. Euro-
507 Mediterranean J Environ Integr 2:. https://doi.org/10.1007/s41207-017-0016-y
508 Othmani A, Kesraoui A, Seffen M (2020b) Removal of phenol from aqueous solution by coupling alternating
509 current with biosorption. Environ Sci Pollut Res. https://doi.org/10.1007/s11356-020-09976-7
510 Pagga U, Brown D (1986) The degradation of dyestuffs: Part II Behaviour of dyestuffs in aerobic biodegradation
511 tests. Chemosphere 15:479–491. https://doi.org/10.1016/0045-6535(86)90542-4
512 Panizza M, Cerisola G (2005) Application of diamond electrodes to electrochemical processes. Electrochim Acta
513 51:191–199. https://doi.org/10.1016/j.electacta.2005.04.023
514 Panizza M, Cerisola G (2009) Direct and mediated anodic oxidation of organic pollutants. Chem Rev 109:6541–
515 6569. https://doi.org/10.1021/cr9001319
516 Perkin E (1996) Analytical Methods for Atomic Absorption Spectroscopy. Anal Methods 216
517 Pogacean F, Rosu M-C, Coros M, et al (2018) Graphene/TiO 2 -Ag Based Composites Used as Sensitive
518 Electrode Materials for Amaranth Electrochemical Detection and Degradation . J Electrochem Soc
519 165:B3054–B3059. https://doi.org/10.1149/2.0101808jes
520 Radhakrishnan S (2014) Roadmap to Sustainable Textiles and Clothing
521 Sasidharan Pillai IM, Gupta AK (2015) Potentiostatic electrodeposition of a novel cost effective PbO2 electrode:
522 Degradation study with emphasis on current efficiency and energy consumption. J Electroanal Chem
523 749:16–25. https://doi.org/10.1016/j.jelechem.2015.04.020
524 Shahryari Z, Goharrizi AS, Azadi M (2010) Experimental study of methylene blue adsorption from aqueous
525 solutions onto carbon nano tubes. Int J Water Resour Environ Eng 2:16–028
526 Silva CP, Marmitt S, Haetinger C, Stülp S (2008) Amaranth food dye photochemical and photoelectrochemical
527 degradation: Experiments and mathematical modelling. WSEAS Trans Syst 7:793–803
528 Singh K, Arora S (2011) Removal of synthetic textile dyes from wastewaters: A critical review on present
529 treatment technologies. Crit Rev Environ Sci Technol 41:807–878.
530 https://doi.org/10.1080/10643380903218376
531 Skoumal M, Arias C, Cabot PL, et al (2008) Mineralization of the biocide chloroxylenol by electrochemical
532 advanced oxidation processes. Chemosphere 71:1718–1729.
533 https://doi.org/10.1016/j.chemosphere.2007.12.029

534 Steter JR, Barros WRP, Lanza MRV, Motheo AJ (2014) Electrochemical and sonoelectrochemical processes
535 applied to amaranth dye degradation. Chemosphere 117:200–207.
536 https://doi.org/10.1016/j.chemosphere.2014.06.085
537 Tran HN, You SJ, Nguyen TV, Chao HP (2017) Insight into the adsorption mechanism of cationic dye onto
538 biosorbents derived from agricultural wastes. Chem Eng Commun 204:1020–1036.
539 https://doi.org/10.1080/00986445.2017.1336090
540 Wang X, Xie Y, Yang G, et al (2020) Enhancement of the electrocatalytic oxidation of antibiotic wastewater
541 over the conductive black carbon-PbO2 electrode prepared using novel green approach. Front Environ Sci
542 Eng 14:. https://doi.org/10.1007/s11783-019-1201-9
543 Zhang G, Yang F, Liu L (2009) Comparative study of Fe2+/H2O2 and Fe3+/H2O2 electro-oxidation systems in
544 the degradation of amaranth using anthraquinone/polypyrrole composite film modified graphite cathode. J
545 Electroanal Chem 632:154–161. https://doi.org/10.1016/j.jelechem.2009.04.010
546 Zhou D, Gao L (2007) Effect of electrochemical preparation methods on structure and properties of PbO2 anodic
547 layer. Electrochim Acta 53:2060–2064. https://doi.org/10.1016/j.electacta.2007.09.005
548

Figures

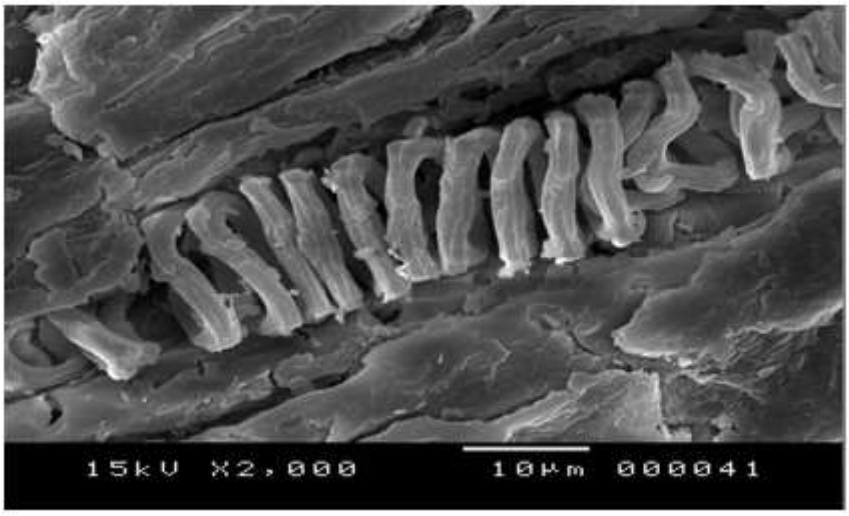

Figure 1

SEM of L.C

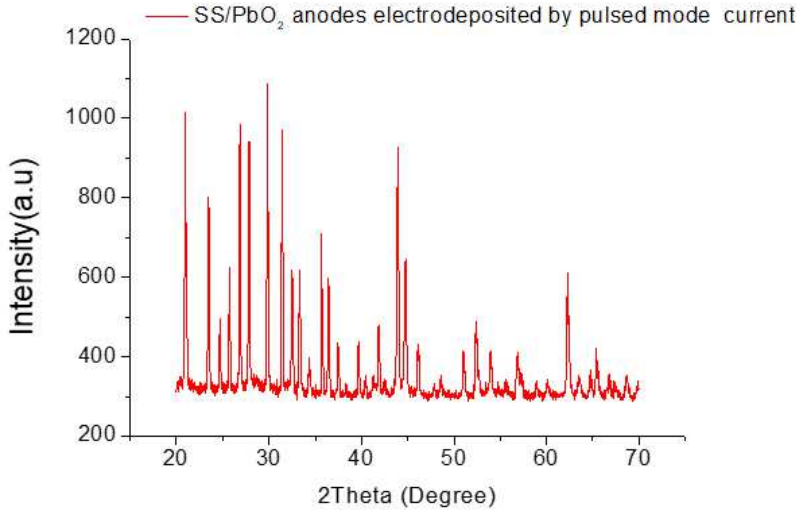

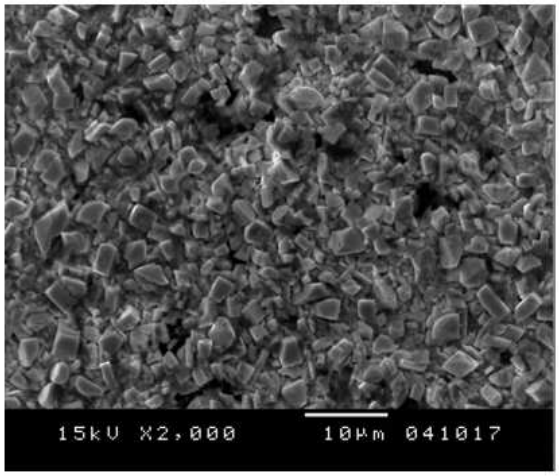

Figure 2

XRD and SEM of SS/PbO2 anodes

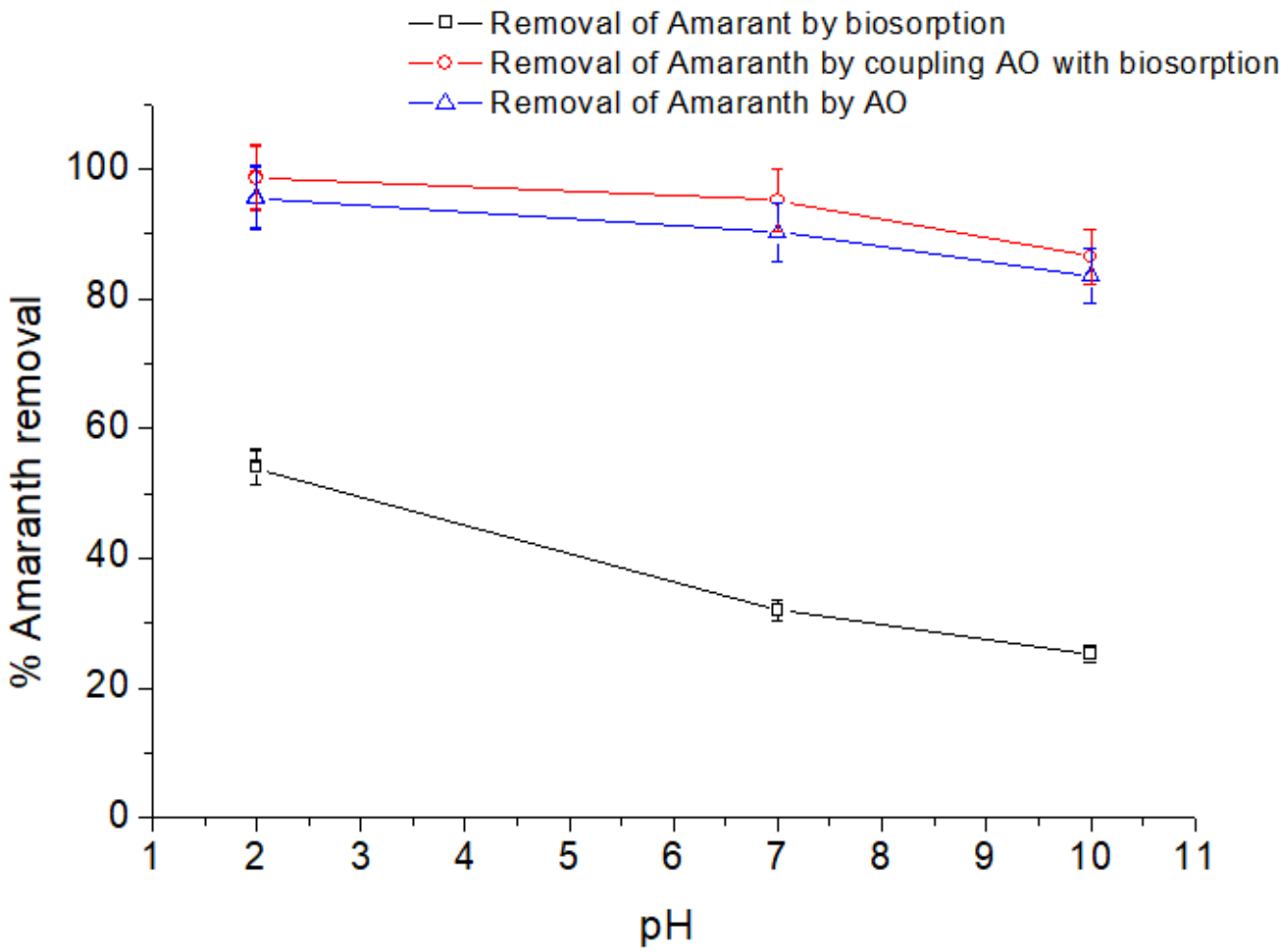

Figure 3

Effect of pH on the removal of Amaranth, C0=10 mg.L-1, t=100 min, T=25°C, CNa2SO4=0.1M, J=25 mA/cm2, m L.C=0.5 g, V=0.5 L

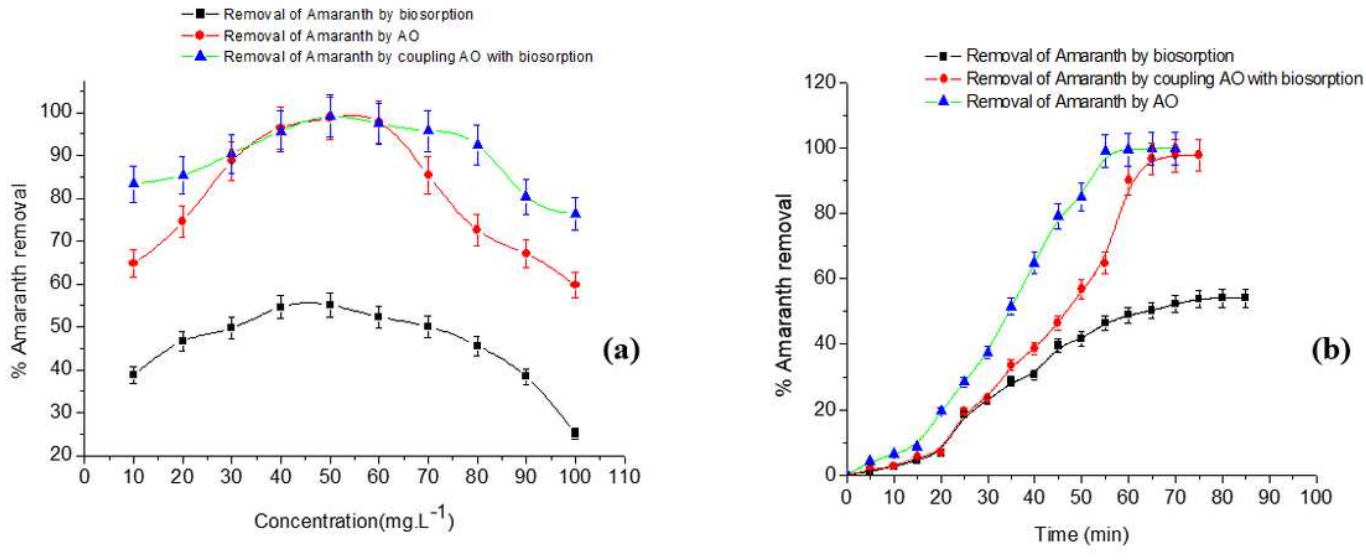

Figure 4

Effect of (a) initial concentration , (b) contact (and electrolysis) time on the removal of Amaranth by biosorption AO, and coupling AO with biosorption, T=25°C, CNa2SO4=0.1M pH=2

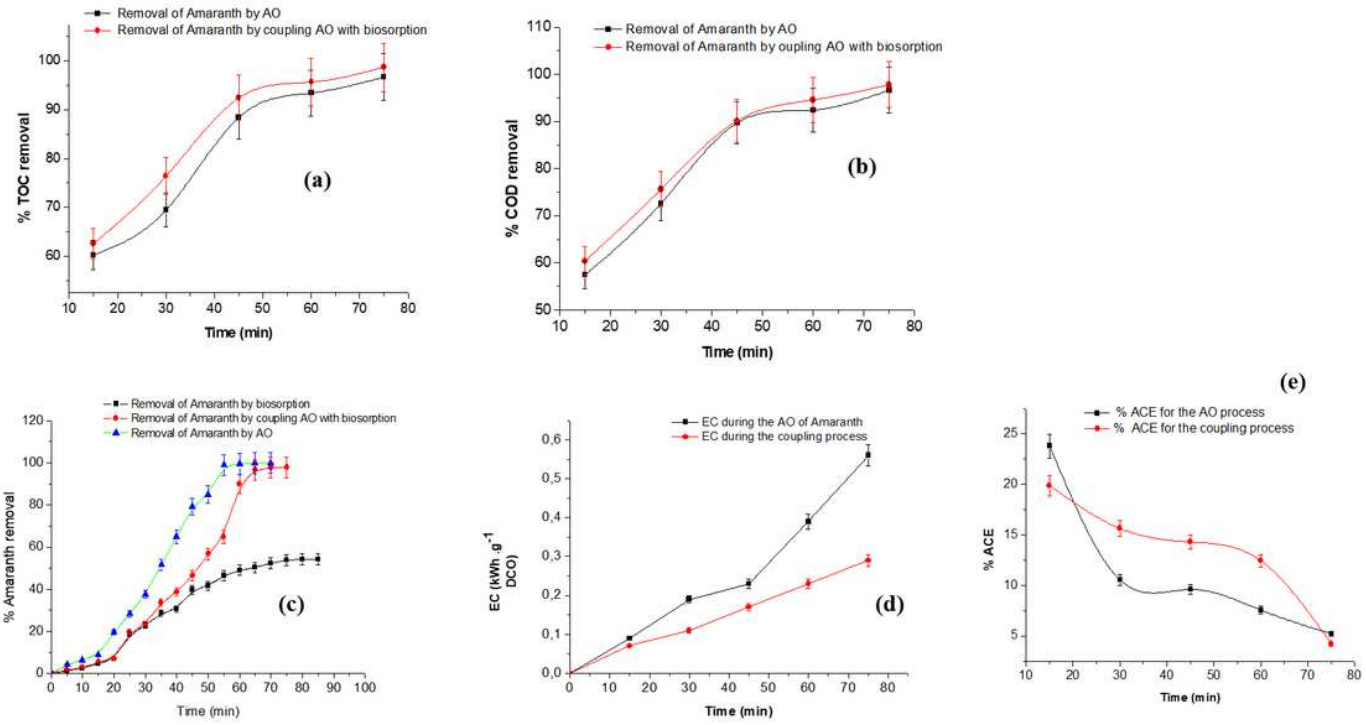

Figure 5

Evaluation of (a) % TOC, (b) % COD; (c) % Amaranth removal , (d) % EC, and (e) %ACE achieved during the removal of Amaranth by AO and coupling AO with C0=10 mg.L-1, J=25 mA.cm-2, T=25°C, CNa2SO4=0.1M, pH=2 , T=80 min

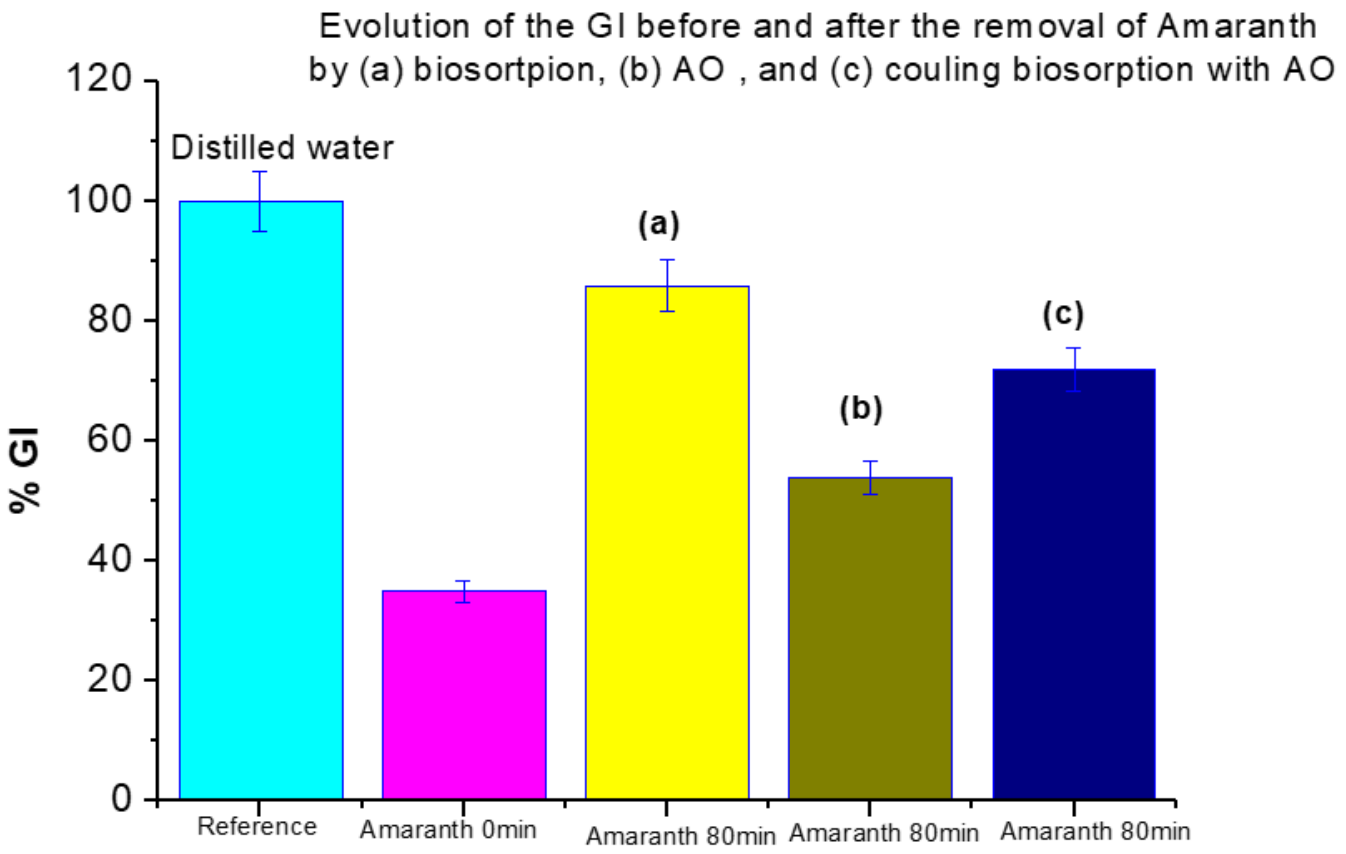

Figure 6

Evolution of the germination index (% GI) before and after removal of Amaranth dye by differ processes

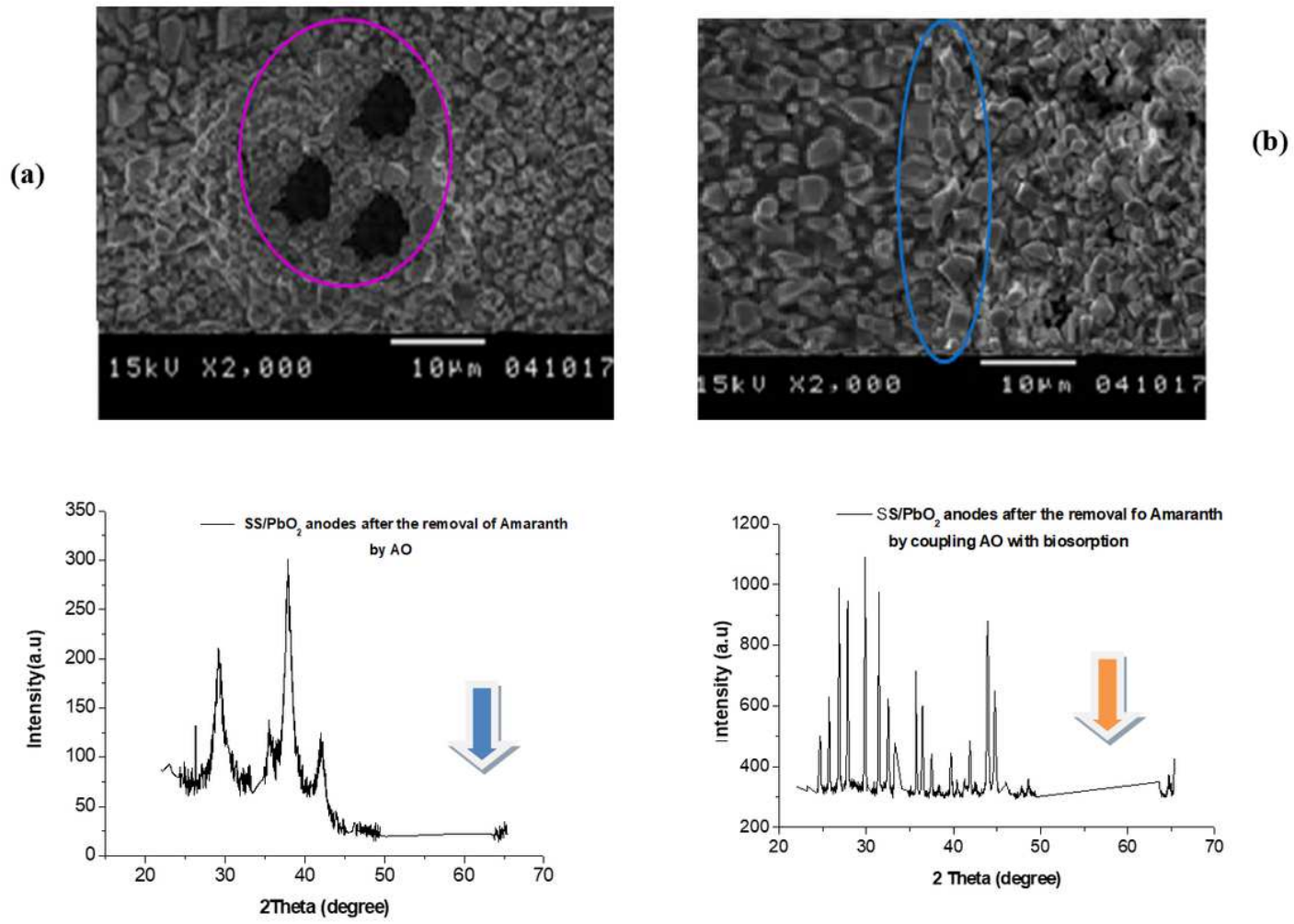

Figure 7

SEM images of SS/PbO2 anodes after the removal of Amaranth dye by (a) AO, (b) coupling AO with biosorption

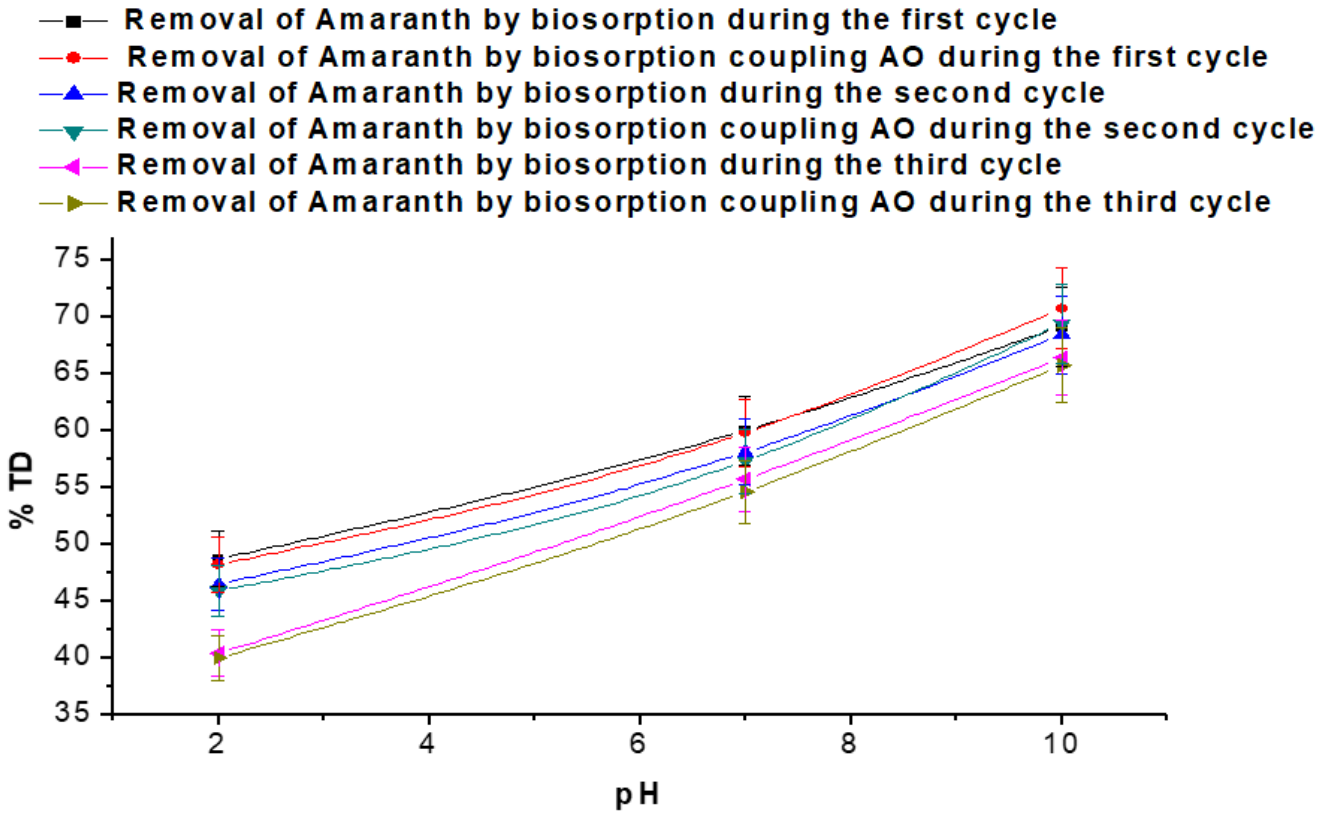

Figure 8

Evaluation of the desorption rate of L.C after the removal of Amaranth dye by AO and AO coupling biosorption after successive cycles (biosorption/desorption)

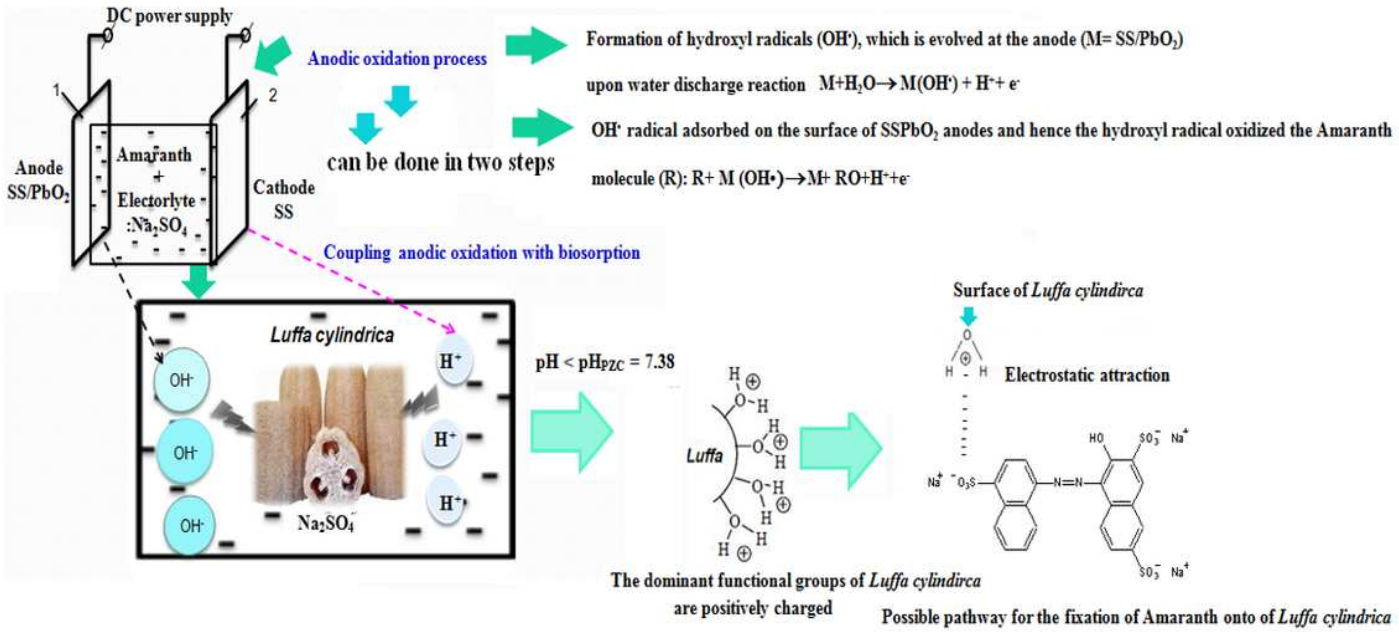

Figure 9

Proposed pathway for the removal of Amaranth by AO and AO coupling biosorption

Supplementary Files

This is a list of supplementary files associated with this preprint. Click to download.

- Supplementarymaterials.docx
- Tables.docx